physica status solidi b
www.pss-b.com
basic solid state physics

Crystal stability and pressure-induced phase transitions in scheelite AWO_4 (A = Ca, Sr, Ba, Pb, Eu) binary oxides. II: Towards a systematic understanding

F. J. Manjón[1], **D. Errandonea**[2], **J. López-Solano**[3], **P. Rodríguez-Hernández**[3], **S. Radescu**[3], **A. Mujica**[3], **A. Muñoz**[3], **N. Garro**[2], **J. Pellicer-Porres**[2], **A. Segura**[2], **Ch. Ferrer-Roca**[2], **R. S. Kumar**[4], **O. Tschauner**[4], and **G. Aquilanti**[5]

[1] Dpto. de Física Aplicada, Univ. Politècnica de València, Cno. de Vera s/n, 46022 València, Spain
[2] Dpto. de Física Aplicada-ICMUV, Univ. de València, c/Dr. Moliner 50, 46100 Burjassot, Spain
[3] Dpto. de Física Fundamental II, Universidad de La Laguna, 38205 La Laguna, Tenerife, Spain
[4] HiPSEC, Univ. of Nevada, 4505 Maryland Parkway, Las Vegas, NV 89154-4002, USA
[5] European Synchrotron Radiation Facility, BP 220, Grenoble, 38043 France

Received 3 July 2006, revised 7 September 2006, accepted 7 September 2006
Published online 15 December 2006

PACS 61.50.Ah, 61.50.Ks, 64.70.Kb

Recent experimental measurements and *ab initio* calculations in scheelite $CaWO_4$, $SrWO_4$, $BaWO_4$, $PbWO_4$, $EuWO_4$ and $YLiF_4$ crystals reveal the existence of complex high-pressure phase diagrams, which present striking differences but also relevant similarities. In this work we show that the high-pressure structural sequence in the studied scheelites can be understood on the basis of the positions of the different ABX_4 compounds in Fukunaga and Yamaoka's diagram and in Bastide's diagram. Our study can help to understand the phase diagrams and high-pressure phase transitions occurring in ABX_4 compounds with scheelite, wolframite, fergusonite, zircon, or pseudoscheelite structures.

phys. stat. sol. (b) **244**, No. 1, 295–302 (2007) / **DOI** 10.1002/pssb.200672588

Original Paper

phys. stat. sol. (b) **244**, No. 1, 295–302 (2007) / **DOI** 10.1002/pssb.200672588

Crystal stability and pressure-induced phase transitions in scheelite AWO_4 (A = Ca, Sr, Ba, Pb, Eu) binary oxides. II: Towards a systematic understanding

F. J. Manjón[*, 1], **D. Errandonea**[2], **J. López-Solano**[3], **P. Rodríguez-Hernández**[3], **S. Radescu**[3], **A. Mujica**[3], **A. Muñoz**[3], **N. Garro**[2], **J. Pellicer-Porres**[2], **A. Segura**[2], **Ch. Ferrer-Roca**[2], **R. S. Kumar**[4], **O. Tschauner**[4], and **G. Aquilanti**[5]

[1] Dpto. de Física Aplicada, Univ. Politècnica de València, Cno. de Vera s/n, 46022 València, Spain
[2] Dpto. de Física Aplicada-ICMUV, Univ. de València, c/Dr. Moliner 50, 46100 Burjassot, Spain
[3] Dpto. de Física Fundamental II, Universidad de La Laguna, 38205 La Laguna, Tenerife, Spain
[4] HiPSEC, Univ. of Nevada, 4505 Maryland Parkway, Las Vegas, NV 89154-4002, USA
[5] European Synchrotron Radiation Facility, BP 220, Grenoble, 38043 France

Received 3 July 2006, revised 7 September 2006, accepted 7 September 2006
Published online 15 December 2006

PACS 61.50.Ah, 61.50.Ks, 64.70.Kb

Recent experimental measurements and *ab initio* calculations in scheelite $CaWO_4$, $SrWO_4$, $BaWO_4$, $PbWO_4$, $EuWO_4$ and $YLiF_4$ crystals reveal the existence of complex high-pressure phase diagrams, which present striking differences but also relevant similarities. In this work we show that the high-pressure structural sequence in the studied scheelites can be understood on the basis of the positions of the different ABX_4 compounds in Fukunaga and Yamaoka's diagram and in Bastide's diagram. Our study can help to understand the phase diagrams and high-pressure phase transitions occurring in ABX_4 compounds with scheelite, wolframite, fergusonite, zircon, or pseudoscheelite structures.

1 Introduction

In the first part of this work [1] we have summarized the results of our experimental and theoretical studies on the high-pressure phase transitions in AWO_4 scheelites (A = Ca, Sr, Ba, Pb, Eu). There are similarities among these scheelites, like the common experimental observation of the fergusonite phase or the predicted stability of orthorhombic phases (like the Cmca phase), but also striking differences, like the absence of a stable $P2_1/n$ phase ($PbWO_4$-III or $BaWO_4$-II-type structure) in $CaWO_4$ or the role played by the fergusonite structure in the phase diagrams. Several experimental and theoretical works on scheelite $YLiF_4$ under pressure have also shown similarities and differences with respect to AWO_4 scheelites (see Ref. [2] and references therein). In view of the seemingly diversity of the emerging picture, we thought that a study of the systematics of the phase transitions in ABX_4 compounds may shed light on their behaviour under compression. In this work, we will show that the observed structures at ambient pressure and their pressure-induced phase transitions in ABX_4 compounds can be understood using Fukunaga and Yamaoka's [3] and Bastide's phase diagrams [4]. Those two works are the latest trials to get a simplified systematics of the crystalline structures observed in ABX_4 compounds and their evolution under pressure. In these diagrams, the structure of a compound at ambient conditions, and consequently its pres-

* Corresponding author: e-mail: fjmanjon@fis.upv.es

sure-induced phase transition, is related to its position in a phase diagram, which in turn is given by the ionic radii ratios of the A and B cations and the X anion.

2 Systematics of the pressure-induced phase transitions

The results summarized in previous papers [1, 2] evidence the existence of common trends in the pressure-induced phase transitions undergone by ABX_4 compounds. In particular, pressure drives structural transformations from tetragonal symmetry to monoclinic symmetry and to orthorhombic symmetry following the structural sequence: zircon-scheelite-(fergusonite or $P2_1/n$)-($BaMnF_4$ or Cmca). A calculation of the ionic radii ratios BX_4/A $[(r_B + r_X)/r_A]$, with r_A being the ionic radius of cation A, r_B being the ionic radius of cation B, and r_X being the ionic radius of anion X, indicates that: zircon (space group [SG] $I4_1/amd$, No. 141, $Z = 4$) and scheelite (SG $I4_1/a$, No. 88, $Z = 4$) structures have BX_4/A ratios between 1.2 and 2.2; monoclinic structures, like fergusonite (SG I2/a, No. 15, $Z = 4$), have ratios from 2.2 to 2.5; and orthorhombic structures, like $BaMnF_4$ (SG $Cmc2_1$, No. 36, $Z = 4$), have ratios above 2.5.

In the 1970's, Fukunaga and Yamaoka studied the systematics of ABO_4 compounds [3] and located the ABO_4 compounds in a diagram with (t, k) coordinates. Coordinate $t = (r_A + r_B)/2r_X$, represents the average cation to anion radii ratio, and coordinate $k = r_A/r_B$ represents the cation A to cation B radii ratio. In the Fukunaga and Yamaoka's (FY) diagram, the ordering of the compounds is based on: 1) the similarities between ABO_4 compounds and AO_2 compounds; 2) the higher coordination (or lower valence) of cation A than cation B; and 3) the possibility of structural changes without increase of cation coordination. In the FY diagram the compounds with the same structure are placed along a diagonal path along the (1,1) direction of the diagram. The pressure-induced phase transitions can be understood if we consider that anions are usually larger and more compressible than cations. Therefore, the normal behaviour of compounds under compression is to undergo phase transitions to more compact structures with larger t values and relatively constant k values, *provided* that steric stresses between cations are small or that anions are far larger than cations [5]. These means that structures in the FY diagram are predicted to undergo pressure-induced phase transitions following the east (E) rule.

In their work, Fukunaga and Yamaoka pointed out an anomaly regarding the high-pressure behaviour of some ABO_4 compounds. $BAsO_4$ and BPO_4 are compounds crystallizing in the high cristobalite structure that undergo a pressure-induced phase transition to quartz. The phase transition in these two compounds does not follow the E rule for pressure increase in the FY diagram. In our opinion, this problem arises due to the wrong location of the high cristobalite compounds of boron in the FY diagram. The wrong location of these two compounds in the FY diagram comes from considering that the valence of the A cation must be lower than the valence of the B cation. We consider that the anomaly in the FY diagram disappears if these two compounds are located in the FY diagram attending to their ionic radii bearing in mind that cation A must be always larger that cation B ($r_A > r_B$). In this case the arsenate and phosphate compounds $BAsO_4$ and BPO_4 must be renamed to become borates $AsBO_4$ and PBO_4. This change of cation ordering is not surprising in boron compounds due to the small radius of boron that lead to boron to have the smaller coordination despite having smaller valence than As or P. In fact, it is known that in BAs and BP there is a reversal of the cation and anion role [6, 7]. Therefore, assuming that these compounds are not arsenates and phosphates but borates, both compounds have $k > 1$ and the phase transition from high cristobalite to quartz is understood. In summary, we think that all ABX_4 compounds can be properly located in the FY diagram provided that $r_A > r_B$; i.e., with $k \geq 1$. In this way the FY diagram can help in understanding the ambient pressure structures and high-pressure phase transitions in a number of ABX_4 compounds.

In the 1980's, Bastide studied the systematics of ABX_4 compounds [4] and located the ABX_4 compounds in a diagram according to coordinates involving their cation-to-anion radii ratios coordinates (r_A/r_X, r_B/r_X). In this way, Bastide's diagram is divided in different $[c_A - c_B]$ regions with c_A and c_B being the coordination of cations A and B, respectively. Figure 1 shows an updated version of Bastide's diagram with the location of the structures which are relevant for the present discussion. The ionic radii of Shannon [8] have been used to locate the compounds in Bastide's diagram.

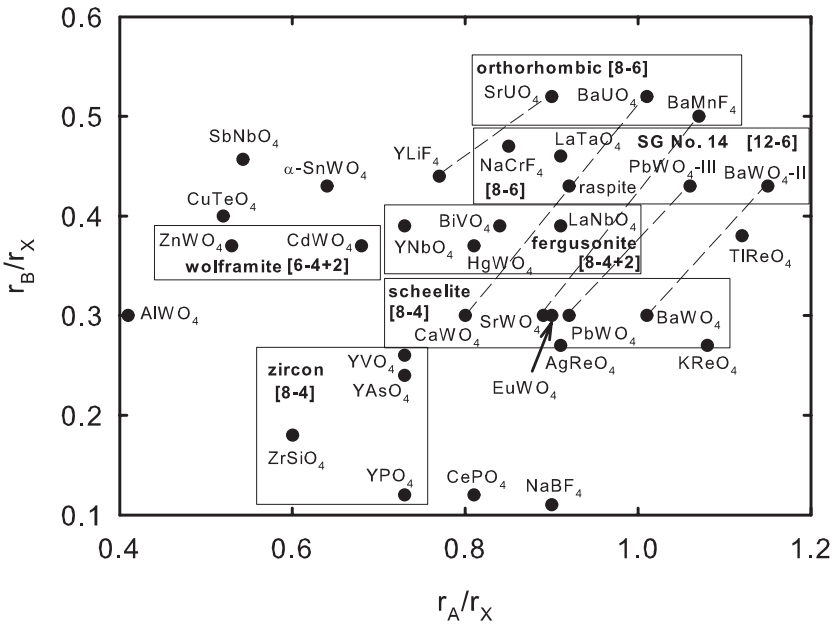

Fig. 1 Updated Bastide's diagram. The dashed lines show the evolution of the ionic radii ratios with increasing pressure in a number of scheelite-structured compounds.

One example of the relaxed cation coordination [$c_A - c_B$] boundaries is scheelite $YLiF_4$ that has [8-4] cation coordination with r_A/r_X and r_B/r_X lying outside the usual stability region of scheelite structures and being even above the limits of the stability of the fergusonite structure. In Bastide's diagram, the normal behaviour under pressure of ABX_4 compounds under compression is to undergo phase transitions to more compacted structures with larger cation-to-anion ionic radii ratios r_A/r_X and r_B/r_X, *provided* that steric stresses between cations are small or that anions are far larger than cations [5]. This normal behaviour leads to the north-east (NE) rule in Bastide's diagram. We show in Fig. 1 that the pressure-induced phase transitions in the ABX_4 compounds studied by us follow closely the NE rule in the Bastide's diagram with increasing pressure.

Like Fukunaga and Yamaoka, Bastide noted that there were some compounds, like those with [12–4] cation coordination, that do not follow the normal NE rule with increasing pressure in Bastide's diagram. High-pressure phases of these compounds tend to increase the cation B coordination without an increase or even a decrease of the cation A coordination; i.e., they follow a north (N) or even a north-west (NW) rule in Bastide's diagram with increasing pressure. This apparent contradiction can be understood if one considers that when the cation A has a much larger radius than the cation B with the cation-A radius being similar or even larger than the anion-X radius, as in [12–4] compounds, the cation A could be as compressible as the anion or even more compressible than the anion, being the cation B almost uncompressible. In this case, the compressed structure of [12–4] compounds tends to undergo a phase transition increasing r_B/r_X but with constant (or even decreasing r_A/r_X); i.e., following a N (or NW) path in Bastide's diagram.

In the following we will analyze the most relevant ABX_4 structures in the light of Bastide's diagram paying attention to their cation coordinations and trying to understand their pressure-induced phase transitions. The tetragonal zircon and scheelite structures are basically the most regular symmetries for ABX_4 compounds with four formula units per unit cell. These structures have [8–4] cation coordination and in Bastide's diagram are approximately located forming a parallelepiped along a diagonal path going from (0.54, 0.12) and (0.72, 0.12) to (0.8, 0.35) and (1.1, 0.35). Compounds with the zircon structure are $ZrSiO_4$, YVO_4, $CdCrO_4$, while compounds with the scheelite structure are the alkaline-earth tungstates and molybdates, $PbMoO_4$, $PbWO_4$, and $EuWO_4$. There are exceptions, like $YLiF_4$ and other scheelite

fluorides, whose r_A/r_X and r_B/r_X ionic radii ratios lie outside the normal scheelite stability region. In general, slight deviations from the above ionic radii ratios lead to structures with orthorhombic, monoclinic or even triclinic symmetry that are deformations of the tetragonal zircon and scheelite structures.

Many orthorhombic structures that are deformations of tetragonal ones, like pseudoscheelite (SG Pnma, No. 62, $Z = 4$), are usually found when r_A is much larger than r_B and are usually located below the zircon-scheelite stability region in the Bastide's diagram. These orthorhombic structures are represented by $TlReO_4$ (1.12, 0.38), $NaBF_4$ (0.9, 0.11), and $InPO_4$ (0.6, 0.11), that crystallize in SGs Nos. 60 to 63. In those structures the cation B has a low coordination. However, there are also less common ABX_4 compounds, like $SrUO_4$, $BaUO_4$ and $PbUO_4$ (SG Pbcm, No. 57, $Z = 4$) [9], that crystallize at ambient conditions in orthorhombic structures with higher cation B coordination. High-density orthorhombic structures like Pbcm and Cmca are located well inside the [8–6] cation coordination region next to the limit for higher cation B coordination, and others, like the $Cmc2_1$ structure of $BaMnF_4$ (1.1, 0.5), have [10–6] cation coordination.

Monoclinic deformations of the zircon and scheelite structures are usually located in the upper side of the zircon-scheelite stability region; i.e., with r_B relatively large compared to r_X and with cation B tending to coordination higher than 4. ABX_4 compounds crystallizing in monoclinic structures belonging to SG No. 12 have between [6–4+2] and [6–4] cation coordination. Those that belong to SG No. 13 have [6–6] cation coordination. Those that belong to SG No. 15 have a [8–4] or [8–4+2] cation coordination and can be viewed as a slight distortion of the scheelite structure. And finally, those that belong to SG No. 14 may have many different cation coordinations such as [6–6], [8–4], [8–6], [12–4], and [12–6]. The large number of different cation coordinations for ABX_4 compounds crystallizing in SG No. 14 justifies that this SG is the monoclinic group symmetry most populated by ABX_4 compounds according to the ICDS database. All the monoclinic structures are located in Bastide's diagram in agreement with their cation coordinations. Monoclinic structures belonging to SG No. 12, like $MgMoO_4$, $AlTaO_4$ and $AlWO_4$ (C2/m, $Z = 8$), are located in the region with [6–4] cation coordination. Curiously, an isomorphous structure to $MgMoO_4$ can be also obtained in $CaWO_4$ at high pressure and high temperature starting from amorphous $CaWO_4$ [10]. The stability region of structures with SG No. 12 is (0.5–0.6, 0.3–0.4). Monoclinic structures with SG No. 13, like the wolframite structure (P2/c, $Z = 2$), are located in the region between [6–4+2] and [6–6] cation coordination and their stability region is (0.5–0.65, 0.35–0.4). Examples are: $AuLiF_4$, $YTaO_4$, $CdWO_4$, $ZnWO_4$, and $FeWO_4$. Monoclinic structures with SG No. 15, like the fergusonite structure, are located in the boundary region between [8–4] and [8–6] cation coordination with a stability region around (0.7–0.95, 0.35–0.4); i.e. just above the zircon-scheelite stability region. Examples are: $YNbO_4$, $NdTaO_4$, $BiVO_4$, and $HgWO_4$. Finally, the monoclinic structures belonging to SG No. 14 are fairly delocalized in Bastide's diagram because of its variety of allowed cation coordinations. There are some compounds in the [8–4] region like monazite ($CePO_4$) and $AgMnO_4$. Other materials are in the [6–6] region like $AlLiCl_4$ and $CuTeO_4$; in the [8–6] region like $NaCrF_4$ and $LaTaO_4$; in the [8–8] region like $RbAuBr_4$; and in the [12–4] region like $RbMnF_4$. Furthermore, $LaTaO_4$ seems to be a compound located near the boundary region between [8–6] and [12–6] cation coordination. Indeed, it has been suggested by recent *ab initio* calculations on $BaWO_4$ [11] that application of pressure leads to a change of cation coordination from [8–6] to [10–6] in the $LaTaO_4$-type structure without change of spatial group. According to this result, the [12–6] border in Bastide's diagram (not printed in Bastide's work) could be located somewhere around $r_A/r_X > 1.1$ and with r_B/r_X around 0.5. Note that in the Bastide's diagram the boundaries between different cation coordination are not strict; one example is the scheelite-structured $YLiF_4$ with [8–4] cation coordination and with r_A/r_X and r_B/r_X ionic radii ratios outside the normal scheelite stability region and above the limits of the fergusonite structure. The location of $LaTaO_4$ structure as a bridge structure between [8–6] and [12–6] cation coordination makes this structure a good candidate for high-pressure phases of a number of zircon and scheelite structures with $r_A \cong 2-3r_B$.

We must note here that there is a region of Bastide's diagram around $r_A/r_X = 1$ and $r_B/r_X = 0.4$ where monoclinic structures with SG No. 14 and No. 15 are rather close. This is the case of $HoTaO_4$ (fergusonite) and $LaTaO_4$ ($P2_1/c$). In fact, one can note that the limits of the monoclinic SG No. 13, 14 and 15 are

overlapped. $YTaO_4$, $HoTaO_4$ and $LaTaO_4$ belong to the monoclinic SG No. 13, 15, and 14, respectively. Furthermore, $YbTaO_4$ has been found in both modifications: monoclinic SG No. 13 and 15. However, $YNbO_4$, $HoNbO_4$ and $LaNbO_4$ crystallize in the fergusonite structure despite the ionic radius of Nb and Ta being similar for the same coordination. These examples illustrate the subtle differences and the diffuse limits of stability of the monoclinic structures with SG No. 13 and No. 15, and of those with SG No. 15 and No. 14 along the same row of "nominally" constant r_B/r_X ratio.

Taking into account the position of different compounds in Bastide's diagram and the application of the NE rule with increasing pressure we can explain the systematics of high-pressure phase transitions occurring in a number of ABX_4 compounds. For instance, $YLiF_4$ (0.78, 0.45) is a compound in the limit of 4-to-6 coordination for Li, that has been predicted to undergo a phase transition from the scheelite to the fergusonite-related M'-fergusonite phase (SG $P2_1/a$, No. 14, $Z = 4$) and afterwards to the Cmca phase (SG Cmca, No. 64, $Z = 8$) [2]. These phase transitions are in agreement with the NE rule. Above the fergusonite region there is a region of phase stability for some monoclinic compounds with structures belonging to SG No. 14 and some orthorhombic compounds (see Fig. 1). In particular, $NaCrF_4$ (0.91, 0.48) and $SrUO_4$ (0.97, 0.69) are compounds crystallizing in the monoclinic M'-fergusonite structure and orthorhombic Pbcm structure at ambient conditions, respectively, both in NE direction with respect to $YLiF_4$. Therefore, the scheelite-monoclinic-orthorhombic transitions proposed for $YLiF_4$ under pressure (see dashed line in Fig. 1) follow reasonably well the NE rule going from scheelite with [8−4] cation coordination to M′-fergusonite with [8−4+2] cation coordination, and afterwards to the Cmca structure with [9-6] cation coordination. It is clear that $YLiF_4$ cannot undergo a phase transition to the fergusonite structure because its cation-to-anion ratios are higher than those of the region of stability of the fergusonite structure and the NE rule does not drive in the direction of fergusonite.

In $CaWO_4$ (0.8, 0.3) and $SrWO_4$ (0.9, 0.3) a transition from the scheelite to the fergusonite structure has been experimentally observed [12], and theoretically confirmed [12, 13]. However, recent *ab initio* calculations provide evidence that the fergusonite and $P2_1/n$ structures are in strong competition in $SrWO_4$ while the fergusonite structure is much more stable in $CaWO_4$ [1]. These phase transitions are in agreement with the NE rule with increasing pressure, because this rule drives $CaWO_4$ and $SrWO_4$ to the region of stability of the fergusonite structure, and beyond it, to the region of stability of the SG No. 14. In $PbWO_4$ (0.92, 0.3) and $BaWO_4$ (1.01, 0.3) calculations have also found a pressure-induced phase transition to the $P2_1/n$ structure [12]. However, a phase transition to the fergusonite structure has been found experimentally in competition with the $P2_1/n$ structure. Again, these phase transitions agree with the NE rule; e.g. $LaNbO_4$ (0.91, 0.39) is a fergusonite-type compound that is above the two structures in N and NE direction, just in the limit of stability of the fergusonite phase, $r_A/r_X = 0.95-1.0$. The competition between fergusonite and $P2_1/n$ phases in the series $CaWO_4$, $SrWO_4$, $PbWO_4$, and $BaWO_4$ is directly related to their r_A/r_X ratio. For smaller r_A/r_X ratios the fergusonite phase dominates over the $P2_1/n$ phase while this last phase dominates over the fergusonite phase in the compounds with larger r_A/r_X ratios. The competition of the $P2_1/n$ structure and the fergusonite structure as a high-pressure phase of $SrWO_4$ can be understood because this compound has $r_{Sr}/r_O = 0.9$ and with increasing pressure the NE rule drives the r_A/r_X ratio to the limit region ($r_{Sr}/r_O = 0.95-1.0$) between SG No. 15 (fergusonite) and SG No. 14 ($P2_1/n$).

Further theoretical transitions have been predicted in the four Ca, Sr, Ba and Pb tungstates, ultimately to the Cmca orthorhombic structure. The Cmca structure has a [9−6] cation coordination and should be located close to the $SrUO_4$, $BaUO_4$ and $BaMnF_4$ structures. On the basis of the similar radii of Eu and Sr, we expect similar phase transitions for $SrWO_4$ and $EuWO_4$. Indeed, in both compounds the appearance of the fergusonite phase was observed at similar pressures [12, 14]. Also due to the similar radii of W and Mo and to the similar location in Bastide's diagram, the same phase transitions of the Ca, Sr, Pb and Ba scheelite tungstates could be expected for the Ca, Sr, Pb, and Ba scheelite molybdates.

As regards the FY diagram, we want to stress that there are striking anomalies that cast reasonable doubts regarding the validity of the E rule for predicting pressure-induced phase transitions. The anomalies of the FY diagram are: 1) Some ABX_4 compounds crystallizing in the scheelite structure are predicted to undergo a phase transition to the wolframite structure under pressure. This is in contradiction with the most recent experiments and with Bastide's diagram where the wolframite structure is not in NE

direction with respect to the scheelite structure. The experimental observation of the scheelite-to-wolframite transition [15, 16] can only be justified under non-hydrostatic conditions that enhance steric stresses leading to the NW rule in Bastide's diagram. 2) ABX_4 compounds crystallizing in the wolframite structure are predicted to undergo a phase transition to fergusonite under pressure. Again, this in is contradiction with Bastide's diagram where the fergusonite structure is not in NE direction with respect to wolframite structure. Instead, a pressure-induced phase transition from wolframite to an orthorhombic structure like the $Pna2_1$ structure (SG No. 33) of $SbNbO_4$, the Pnna structure (SG no. 52) of α-$SnWO_4$, the Pbcm structure (SG No. 57) of $SrUO_4$, or the predicted high-pressure Cmca phase of $CaWO_4$ could be feasible. On the light of these anomalies of the FY diagram, we consider that Bastide's diagram is more convenient than the FY diagram in order to predict high-pressure phases of ABX_4 compounds.

Finally, it must be noted that the zircon-to-scheelite phase transition also follows the NE rule with increasing pressure. Scheelites, like $CaWO_4$ (0.8, 0.3), are in NE direction with respect to zircon compounds, like YVO_4 (0.72, 0.26). Indeed according to our calculations, zircon-type structures become stable at expanded volumes (and corresponding *negative* pressures) in all the compounds studied (see Fig. 1). The zircon-scheelite-fergusonite sequence has been also recently predicted theoretically for $YCrO_4$ [17] and $CaCrO_4$ [18] and has been recently observed experimentally in $YCrO_4$ [19] and $ZrSiO_4$ [20]. Therefore, the systematics here presented can be useful for predicting post-scheelite phases in compounds isostructural to zircon.

3 Pressure-induced amorphization, decomposition and size criterion

In the previous section we have explained that phase transitions to denser crystalline phases take place usually in ABX_4 compounds when they obey the E rule in the FY diagram or the NE rule in Bastide's diagram. However, these rules for increasing pressure are not obeyed when the increase of pressure leads to the dominance of the steric repulsion over the decrease of ionic radii. In that case, pressure can lead to denser amorphous phases or even to the decomposition of the compound into several constituents. Clear evidence of pressure-induced amorphization in ABX_4 compounds has been observed in $CaWO_4$ above 40 GPa [16], in $BaWO_4$ above 47 GPa [11], in $YCrO_4$ above 29 GPa [19], and in the scheelite-structured dimolybdate $NaLa(MoO_4)_2$ above 30 GPa [21]. On the other hand, pressure-induced decomposition has been found in $SrWO_4$ above 15 GPa [22] and in $GdLiF_4$ [23]. Additionally, in $PbWO_4$ an important increase of the disorder of the crystalline structure is observed above 10 GPa [11]. Recent studies in A_2BX_4 compounds [24] show that pressure-induced amorphization can be understood in terms of the packing of the anionic BX_4 units around the A cations (size criterion) and suggest that the A_2BX_4 compounds tend to amorphization when $(r_B + r_X)/r_A$ ratio is higher than 1.43, or equivalently when $r_B/r_X > 1.43 r_A/r_X - 1$. It remains to be checked whether this size criterion can be applied for ABX_4 compounds. If this is the case this would mean that $CaWO_4$, $SrWO_4$, and $EuWO_4$ should tend to amorphization while $PbWO_4$ and $BaWO_4$ should not.

A size criterion effect deduced for A_2BX_4 compounds that has been already checked for ABX_4 compounds is the linear relationship existing between the pressure at which the first phase transition occurs and the packing ratio of the anionic BX_4 units around the A cation [25]. Since the proposal of this size criterion several ABX_4 compounds like $GdLiF_4$ [23], $BaMoO_4$ [26], $LuLiF_4$ [27], and YVO_4 [28] have been found to agree with it. Another size criterion that also seems to be confirmed for ABX_4 compounds in the last years is the linear relationship existing between the bulk modulus and the charge density in the AX_8 polyhedra [12]. In particular, our estimations for the bulk modulus of the hardest ABO_4 compounds, like $ZrSiO_4$, $ZrGeO_4$ and $HfGeO_4$ have been clearly confirmed [29].

4 Concluding remarks

We have studied the pressure behaviour of scheelite tungstates and found that they undergo structural transitions that can be understood with the help of Bastide's diagram. The systematics can be extended to other ABX_4 compounds, like wolframites, fergusonites, scheelite perrhenates ($AgReO_4$) and molybdates,

pseudoscheelite perrhenates ($TlReO_4$), and zircon-type compounds ($ZrSiO_4$). Furthermore, the systematics can be used to predict the high-pressure behaviour of several minerals in the Earth's upper mantle. We have to note that one must be careful when using Fukunaga and Yamaoka's or Bastide's diagrams for predicting high-pressure phases because the exact location of the compounds in the diagrams, and consequently their high-pressure phases, depends on the cationic radii which in turn depends on the cation coordination (that sometimes is not known). Furthermore, we have to note that the ordering of ABX_4 compounds in BX_4 families, as shown in Fukunaga and Yamaoka's [3] and in Bastide's [4] diagrams, can be misleading since the same B cation may have different ionic radii depending on its coordination. Therefore, the BX_4 families are orientative and only valid for those compounds with a B cation with the same coordination and consequently the same ionic radius. The size criterion has been applied with success to ABX_4 compounds and needs to be explored further in order to determine the conditions for pressure-induced amorphization or decomposition. The systematics discussed along the paper can be a helpful tool to improve the understanding of the pressure effects on the electronic and luminescence properties of ABX_4 compounds [30–34].

Acknowledgements This study was made possible through financial support from the Spanish MCYT under grants Nos. MAT2002-04539-CO2-01/-02 and MAT2004-05867-C03-03/-01 and by the Generalitat Valenciana (ACOMP06/181). We thank the APS, NSLS and ESRF for the provision of synchrotron radiation facilities. F.J.M. acknowledges the financial support from the "Programa de Incentivo a la Investigación" of the Universidad Politécnica de Valencia. D.E. and N.G. acknowledge the financial support from the MCYT of Spain through the "Ramón y Cajal" program.

References

[1] J. López-Solano, P. Rodríguez-Hernández, S. Radescu, A. Mujica, A. Muñoz, D. Errandonea, F. J. Manjón, J. Pellicer-Porres, N. Garro, A. Segura, Ch. Ferrer-Roca, R. S. Kumar, O. Tschauner, and G. Aquilanti, phys. stat. sol. (b) **244**, 325 (2007) (this issue).
[2] J. López-Solano, P. Rodríguez-Hernández, A. Muñoz, and F. J. Manjón, Phys. Rev. B **73**, 094117 (2006).
[3] O. Fukunaga and S. Yamaoka, Phys. Chem. Miner. **5**, 167 (1979).
[4] J. P. Bastide, J. Solid State Chem. **71**, 115 (1987).
[5] A. W. Sleigth, Acta Cryst. B **28**, 2899 (1972).
[6] G. W. L. Hart and A. Zunger, Phys. Rev. B **62**, 13522 (2000).
[7] M. J. Herrera-Cabrera, Ph.D. Thesis, unpublished.
[8] R. D. Shannon, Acta Cryst. A **32**, 751 (1976).
[9] L. E. Depero and L. Sangaletti, J. Solid State Chem. **129**, 82 (1997).
[10] D. Errandonea, M. Somayazulu, and D. Häusermann, phys. stat. sol. (b) **231**, R1 (2002).
[11] D. Errandonea, J. Pellicer-Porres, F. J. Manjón, A. Segura, Ch. Ferrer-Roca, R. S. Kumar, O. Tschauner, P. Rodríguez-Hernández, J. López-Solano, S. Radescu, A. Mujica, A. Muñoz, and G. Aquilanti, Phys. Rev. B **73**, 224103 (2006).
[12] D. Errandonea, J. Pellicer-Porres, F. J. Manjón, A. Segura, Ch. Ferrer-Roca, R. S. Kumar, O. Tschauner, P. Rodríguez-Hernández, J. López-Solano, S. Radescu, A. Mujica, A. Muñoz, and G. Aquilanti, Phys. Rev. B **72**, 174106 (2005).
[13] P. Rodríguez-Hernández, J. López-Solano, S. Radescu, A. Mujica, A. Muñoz, D. Errandonea, J. Pellicer-Porres, A. Segura, Ch. Ferrer-Roca, F. J. Manjón, R. S. Kumar, O. Tschauner, and G. Aquilanti, J. Phys. Chem. Solids **67**, 2164 (2006).
[14] D. Errandonea, phys. stat. sol. (b) **242**, R125 (2005).
[15] M. Nicol and J. F. Durana, J. Chem. Phys. **54**, 1436 (1971).
[16] D. Errandonea, M. Somayazulu, and D. Häussermann, phys. stat. sol. (b) **235**, 162 (2003).
[17] L. Li, W. Yu, and Ch. Jin, Phys. Rev. B **73**, 174115 (2006).
[18] Y. W. Long, L. X. Yang, S. Y. You, Y. Yu, R. C. Yu, C. Q. Jin, and J. Liu, J. Phys.: Condens. Matter **18**, 2421 (2006).
[19] Y. W. Long, L. X. Yang, Y. Yu, F. Y. Li, R. C. Yu, S. Ding, Y. L. Liu, and C. Q. Jin, Phys. Rev. B **74**, 054110 (2006).
[20] H. P. Scott, Q. Williams, and E. Knittle, Phys. Rev. Lett. **88**, 015506 (2002).

[21] A. Jayaraman, S. Y. Wang, S. R. Shieh, S. K. Sharma, and L. C. Ming, J. Raman Spectrosc. **26**, 451 (1995).
[22] A. Grzechnik, W. A. Chrichton, and M. Hanfland, phys. stat. sol. (b) **242**, 2795 (2005).
[23] A. Grzechnik, W. A. Chrichton, P. Bouvier, V. Dmitriev, H. P. Weber, and J. Y. Gesland, J. Phys.: Condens. Matter **16**, 7779 (2004).
[24] G. Serghiou, H. Reichmann, and R. Boehler, Phys. Rev. B **55**, 14765 (1997).
[25] D. Errandonea, F. J. Manjón, M. Somayazulu, and D. Häusermann, J. Solid State Chem. **177**, 1087 (2004).
[26] V. Panchal, N. Garg, and S. M. Sharma, J. Phys.: Condens. Matter **18**, 3917 (2006).
[27] A. Grzechnik, K. Friese, V. Dmitriev, H. P. Weber, J. Y. Gesland, and W. A. Crichton, J. Phys.: Condens. Matter **17**, 763 (2005).
[28] X. Wang, I. Loa, K. Syassen, M. Hanfland, and B. Ferrand, Phys. Rev. B **70**, 064109 (2004).
[29] V. Panchal, N. Garg, S. N. Achari, A. K. Tyagi, and S. M. Sharma, J. Phys.: Condens. Matter **18**, 8241 (2006).
[30] D. Errandonea, D. Martínez-García, R. Lacomba-Perales, J. Ruiz-Fuertes, and A. Segura, Appl. Phys. Lett. **89**, 091913 (2006).
[31] D. Errandonea, Ch. Tu, G. Jia, I. R. Martin, U. R. Rodríguez-Mendoza, F. Lahoz, M. E. Torres, and V. Lavin, to appear in J. Alloys Compd. (2007).
[32] F. J. Manjon, S. Jand, G. Riou, B. Ferrand, and K. Syassen, Phys. Rev. B **69**, 165121 (2004).
[33] F. J. Manjon, S. Jandl, K. Syassen, and J. Y. Gesland, Phys. Rev. B **64**, 235108 (2001).
[34] J. López-Solano, P. Rodríguez-Hernández, A. Muñoz, and F. J. Manjón, J. Phys. Chem. Solids **67**, 2077 (2006).

